

Interference and SINR coverage in spatial non-slotted Aloha networks

Barłomiej Błaszczyszyn
Inria/ENS
Paris FRANCE
Bartek.Blaszczyszyn@ens.fr

Paul Mühlethaler
Inria Rocquencourt
Le Chesnay FRANCE
Paul.Muhlethaler@inria.fr

Abstract: In this paper we propose two analytically tractable stochastic-geometric models of interference in ad-hoc networks using pure (non-slotted) Aloha as the medium access. In contrast the slotted model, the interference in pure Aloha may vary during the transmission of a tagged packet. We develop closed form expressions for the Laplace transform of the empirical average of the interference experienced during the transmission of a typical packet. Both models assume a power-law path-loss function with arbitrarily distributed fading and feature configurations of transmitters randomly located in the Euclidean plane according to a Poisson point process. Depending on the model, these configurations vary over time or are static. We apply our analysis of the interference to study the Signal-to-Interference-and-Noise Ratio (SINR) outage probability for a typical transmission in pure Aloha. The results are used to compare the performance of non-slotted Aloha to the slotted one, which has almost exclusively been previously studied in the same context of mobile ad-hoc networks.

Index Terms—Pure (non-slotted) Aloha, Slotted Aloha, SINR, Shot-Noise, MAC Layer Optimization, Throughput, Stochastic geometry, Poisson point process.

I. INTRODUCTION

Aloha is one of the simplest multiple access communication protocols. The main idea is that sources, independently of each other, transmit packets and back-off for random times before the next transmission. A classical model of Aloha assumes that when two or more transmissions overlap in time then neither of them is successful (a collision occurs). This simple model is not adequate in the wireless context. Indeed, the geometry of nodes in the network may allow some simultaneous transmissions to be successful due to the capture (or spatial reuse) effect. Since 1988 and the seminal paper [10], new models have been developed to describe Aloha networks with spatial reuse and capture effect. The model proposed in [4], which inspired our work, falls into this category. To the best of our knowledge, almost all of these studies use slotted Aloha, except [8], which we revisit in this paper. In Section II, we consider a wireless ad-hoc network modeled by homogeneous Poisson point process. We assume power-law decay of the signal in the path-loss model as well as a general distribution of the

fading. We consider two models for non-slotted Aloha: the *Poisson rain* model with dynamic node activation and the *Poisson renewal* model with a static positioning of nodes. In both of these models, we characterize the Laplace transform of the distribution of the empirical average of the interference received during the reception of a typical packet, see Section III. The expressions are particularly simple for the *Poisson rain* model. Next in Section IV, we use this characterization of the Laplace transform of the interference to express the probability of a successful transmission in pure Aloha. Finally, we optimize and compare space-time and energy efficiency of pure Aloha with the previously studied performance of slotted Aloha (Subsection IV-B). We show that the *Poisson rain* and the *Poisson renewal* models provide comparable results and that the *Poisson renewal* model converges towards the *Poisson rain* model when the node density increases.

Comparison of slotted and non-slotted Aloha is a classical subject. In a simple but widely used model where the aggregate packet transmission process follows a Poisson distribution (i.e the spatial reuse is not taken into account) pure (*non-slotted*) Aloha can on average attain the fraction $1/(2e) \approx 18.4\%$ of successful transmissions, when the scheme is optimized by tuning the mean back-off time. It can be shown that this performance can be multiplied by 2 in *slotted-Aloha*, when all the nodes are synchronized and can send packets only at the beginnings of some universal time slots. In this paper we show that taking into account the spatial distribution of transmitters makes the comparison of both types of Aloha more subtle. Specifically, we observe that when the path-loss exponent is not very strong both Aloha protocols, when appropriately optimized, exhibit a similar performance (see Figure 4). Hence the extra complexity required by slotted Aloha may be questionable. For stronger path-loss, slotted Aloha offers a gain (due to synchronisation), which is however much smaller than that predicted by the classical (geometry-less) models of Aloha, which do not take into account the spatial reuse effect but assume collisions for all simultaneously transmitted packets. Moreover, we observe in all path-loss scenarios that both slotted and pure Aloha schemes exhibit the same energy efficiency

(see Subsection IV-C).

The results presented in this paper allow the performance of slotted and non-slotted Aloha with spatial reuse to be evaluated directly (or indirectly via numerical computations). The tools introduced in this paper can handle various fading scenarios. Although the mainstream protocols currently used are based on the Carrier Sense Multiple Access (CSMA) scheme, we know that these protocols do not always work satisfactorily. For instance, we know that the hidden-terminal problem is a very serious issue for CSMA, which, in such a situation, behaves at most no better than an Aloha protocol. Tuning the carrier sense threshold of CSMA is also very difficult when the node density of the network varies greatly. In these situations Aloha protocols can be a perfectly acceptable alternative to CSMA protocols. In all our Aloha models the back-off is taken into account via the medium access probability or explicit back-off times.

A. Related Work

The shot noise process formed from a sum of response functions of a Poisson process and identically distributed random variables was already studied back in the 60s, cf [11]. The first attempts to study interference using the Laplace transforms of the shot noise can be found in [15, 17]. In [13] the shot noise created in a Poisson process with a power-law path-loss function was studied and observed to have a stable distribution.

In [4] the authors introduce what is today called the Poisson bipolar model of an ad-hoc network and using the Laplace transform of the interference they calculate the SINR capture probability for a typical packet transmission in the slotted Aloha MAC. This approach has been next extended.

In [12] the outage probability of a packet in a Signal-over-Interference-Ratio model is extensively investigated. This paper considers many situations: Poisson point process and deterministic node placement. Various kinds of fading are studied. The study also varies the medium access scheme considering Aloha and Time Division Multiple Access (TDMA). The author computes the outage probability of a packet in all these situations. In [5] a channel-fading opportunistic Aloha is considered.

Most research papers on Aloha and its performance concern slotted Aloha. Very few papers study pure (non-slotted) Aloha. The early papers on pure Aloha such as [14] do not consider spatial reuse. The present paper, inspired by the original approach of [4], revisits and extends the study of pure Aloha proposed in [8].

The remaining part of this paper is organized as follows. Section II describes the two models for pure Aloha: the *Poisson rain* and the *Poisson renewal* models. Section III analyzes the interference in our Aloha

networks by computing the Laplace transform of the mean interference for pure Aloha in the *Poisson rain* and the *Poisson renewal* models for a general fading. In Section IV, we study the SINR coverage probability using the Laplace transform of the empirically averaged interference. We can thus optimize pure Aloha and compare the performance with the slotted version of the protocol. Section V contains the simulation results which validate our models and also provides numerical comparisons of slotted and pure Aloha. Section VI concludes the paper. The appendix provides the computation of the Laplace transform of the mean interference with pure Aloha in the *Poisson renewal* model. This computation is somewhat technical, which is why we include it in the Appendix.

II. NETWORK AND ALOHA MODEL

In this section we present our models of non-slotted Aloha for wireless ad-hoc networks. To facilitate future comparisons, we also recall the basic spatial slotted Aloha model.

A. Location of Nodes — The Spatial Poisson Bipolar Network Model

We consider a *Poisson bipolar network model* in which each point of the Poisson pattern represents a node of a Mobile Ad hoc NETWORK (MANET) and is hence a potential transmitter. Each node has an associated receiver located at distance r . This receiver is not part of the Poisson pattern of points. Using the formalism of the theory of point processes, we will say that a snapshot of the MANET can be represented by an independently marked Poisson point process (P.p.p) $\tilde{\Phi} = \{(X_i, y_i)\}$, where the *locations of nodes* $\Phi = \{X_i\}$ form a homogeneous P.p.p. on the plane, with an intensity of λ nodes per unit of space, and where the mark y_i denotes the location of the receiver for node X_i . We assume here that no two transmitters have the same receiver and that, given Φ , the vectors $\{X_i - y_i\}$ are i.i.d with $|X_i - y_i| = r$. In this paper r is constant however, in principle, the results obtained can be extended by integrating the final formulas with an arbitrary distribution of r by in. However more realistic models would require the joint study of routing and MAC, which is beyond the scope of this paper.

B. Aloha Models — Time Added

We will now consider two time-space scenarios appropriate for slotted and non-slotted Aloha. In both of them the planar locations of MANET nodes and their receivers $\tilde{\Phi}$ remain fixed. It is the medium access control (MAC) status of these nodes that will evolve differently over time depending on which of the following two models is used.

1) *Slotted Aloha*: In this model we assume that the time is discrete, i.e. divided into slots of length B (the analysis will not depend on the length of the time-slot) and labeled by integers $n \in \mathbb{Z}$. The nodes of Φ are *perfectly synchronized* to these (universal) time slots and send packets according to the following *slotted Aloha policy*: each node, at each time slot independently tosses a coin with some bias p which will be referred to as the *medium access probability (MAP)*; it sends the packet in this time slot if the outcome is heads and backs off its transmission otherwise. This evolution of the MAC status of each node X_i can be formalized by introducing its further (multi-dimensional) mark $(e_i(n) : n \in \mathbb{Z})$, where $e_i(n)$ is the medium access indicator of node i at time n ; $e_i(n) = 1$ if node i is allowed to transmit in the time slot considered and 0 otherwise. Following the Aloha principle we assume that $e_i(n)$ are i.i.d. (in n and i) and independent of everything else, with $\mathbf{P}(e_i(n) = 1) = p$. We treat p as the main parameter to be tuned for slotted Aloha. We will call the above case *the slotted Aloha model*.

2) *Poisson-renewal Model of Non-slotted Aloha*: In this *non-slotted Aloha* model all the nodes of Φ independently, without synchronization, send packets of the same duration B and then back off for some random time. This can be integrated in our model by introducing marks $(T_i(n) : n \in \mathbb{Z})$, where $T_i(n)$ denotes the beginning of the n th transmission of node X_i with $T_i(n+1) = T_i(n) + B + E_i(n)$, where $E_i(n)$ is the duration of the n th back-off time of node X_i . The non-slotted Aloha principle states that $E_i(n)$ are i.i.d. (in i and n) independent of everything else. In what follows we assume that $E_i(n)$ are exponential with mean $1/\epsilon$ and will consider the parameter ϵ as the main parameter to be tuned for non-slotted Aloha (given the packet transmission time B). More precisely, the lack of synchronization of the MAC mechanism is reflected in the assumption that the temporal processes $(T_i(n) : n \in \mathbb{Z})$ are time-stationary and independent (for different i). Note also that these processes are of the *renewal* type (i.e., have i.i.d. increments $T_i(n+1) - T_i(n)$). For this reason we will call this case the *Poisson-renewal model for non-slotted Aloha*. The MAC state of node X_i at (real) time $t \in \mathbb{R}$ can be described by the on-off process $e_i^{\text{renewal}}(t) = \mathbf{1}(T_i(n) \leq t < T_i(n) + B$ for some $n \in \mathbb{Z}$).

C. Fading and External Noise

We need to complete our network model by some radio channel conditions. We will consider the following *fading scenario*: channel conditions vary from one transmission to another and between different emitter-receiver pairs, but remain fixed for any given transmission. To include this in our model, we assume a further multidimensional

mark $(\mathbf{F}_i(n) : n \in \mathbb{Z})$ of node X_i where $\mathbf{F}_i(n) = (F_i^j(n) : j)$ with $F_i^j(n)$ denoting the *fading* in the channel from node X_i to the receiver y_j of node X_j during the n th transmission. We assume that $F_i^j(n)$ are i.i.d. (in i, j, n) and independent of everything else. Let us denote by F the generic random variable of the fading. We always assume that $0 < \mathbf{E}[F] = 1/\mu < \infty$. In the special case of Rayleigh fading, F is exponential (with parameter μ). (see e.g. [16, pp. 50 and 501]). We can also consider non-exponential cases, which allow other types of fading to be analyzed, such as e.g. Rician or Nakagami scenarios or simply the case without any fading (when $F \equiv 1/\mu$ is deterministic).

In addition to fading we consider a non-negative random variable W independent of $\tilde{\Phi}$ modeling the power of the external (thermal) noise. The Laplace transform of W will be denoted by $\mathcal{L}_W(s) = \mathbf{E}[e^{-sW}]$. (More generally, we denote by $\mathcal{L}_U(\xi)$ the Laplace transform of a random variable U .)

The slotted Aloha model described above, when considered in a given time slot, coincides with the Poisson Bipolar model with independent fading considered in [4]. It allows one to derive a simple, explicit evaluation of the successful transmission probability and other characteristics such as the density of successful transmissions, the mean progress, etc.

An exact analysis of the Poisson-renewal non-slotted Aloha model, albeit feasible, does not lead to similarly closed form expressions. To improve upon this situation, in what follows we propose another model for the non-slotted case. It allows the results to be as explicit as those of [5], which are moreover very close to those of the Poisson-renewal model in a high node density regime.

D. Poisson Rain Model for Non-slotted Aloha

The main difference with respect to the scenario considered above is that the nodes X_i and their receivers y_i are not fixed in time. Rather, we consider a time-space Poisson point process $\Psi = \{(X_i, T_i)\}$ with $X_i \in \mathbb{R}^2$ denoting the location of the emitter which sends a packet during time interval $[T_i, T_i + B)$ (indexing by i is arbitrary and in particular does not mean successive transmissions over time). We may think of node X_i as being “born” at time T_n transmitting a packet during time B and “disappearing” immediately after. Thus the MAC state of the node X_i at (real) time $t \in \mathbb{R}$ is simply $e_i(t) = \mathbf{1}(T_i \leq t < T_i + B)$.

We always assume that Ψ is homogeneous (in time and space) P.p.p. with intensity λ_s . This parameter corresponds to the *space-time frequency of channel access*; i.e., the number of transmission initiations per unit of space and time. The points (X_i, T_i) of the space-time P.p.p. Ψ are marked by the receivers y_i in the same manner as

described in Section II-A; i.e, given Ψ , $\{X_i - y_i\}$ are i.i.d random vectors with $|X_i - y_i| = r$.

This Poisson Rain model is obviously appropriate when the nodes are moving very fast, thus at each transmission it is as if the locations of all the nodes are re-sampled. Although this model does not generally cover our networks, we will show that the Poisson Rain model leads to closed formulas and performs similarly to the usual model where the locations of nodes are not re-sampled at each transmission.

Moreover, they are marked by $\mathbf{F}_i = (F_i^j : j)$, with F_i^j denoting the fading in the channel from X_i to the y_j (meaningful only if X_i, X_j coexist for a certain time). We assume that $F_i^j(n)$ are i.i.d. (in i, j) and of everything else, with the same generic random fading F as in Section II-C. We will call the above model the *Poisson rain model for non-slotted Aloha*. It can be naturally justified by the *mobility of nodes*.

For all the models that we have preented we define the channel access probability τ as the probability that a given node transmits a packet a given time. In the slotted model $\tau = p$, in the non-slotted Poisson renewal model $\tau = \frac{B}{B+1/\epsilon}$. In the non-slotted Poisson rain model we have $\tau = \tau_s/\lambda$.

III. INTERFERENCE ANALYSIS

A. Path-loss Model

Let us assume that all transmitters, when authorized by Aloha, emit packets with unit signal power and that the receiver y_i of node X_i receives the power from the node located at X_j (provided this node is transmitting) equal to $F_j^i/l(|X_j - y_i|)$, where $|\cdot|$ denotes the Euclidean distance on the plane and $l(\cdot)$ is the path loss function. An important special case consists in taking

$$l(u) = (Au)^\beta \quad \text{for } A > 0 \text{ and } \beta > 2. \quad (3.1)$$

Other possible choices of path-loss function avoiding the pole at $u = 0$ consist in taking e.g. $\max(1, l(u))$, $l(u+1)$, or $l(\max(u, u_0))$.

By interference we understand the sum of the signal powers received by a given receiver from all the nodes transmitting in the network except the receiver's own transmitter.

B. Interference

1) *Slotted Aloha* : Let us denote by $I_i(n)$ the *interference* at receiver y_i at time n ; i.e., *the sum of the signal powers received by y_i from all the nodes in $\Phi^1(n) = \{X_j \in \Phi : e_j(n) = 1\}$ except X_i , namely,*

$$I_i(n) = \sum_{X_j \in \Phi^1(n), j \neq i} F_j^i(n)/l(|X_j - y_i|). \quad (3.2)$$

2) *Non-slotted Aloha*: When transmissions are not synchronized (as is the case for non-slotted Aloha) the interference *may vary during a given packet transmission* because other transmissions may start or terminate during it. In our Poisson-renewal model of Section II-B2 this interference process $I_i(n, t)$ during the n th transmission to node y_i can be expressed using (3.2) with $\Phi^1(n)$ replaced by $\Phi_{ren}^1(t) = \{X_j \in \Phi : e_j^{ren}(t) = 1\}$. Similarly, in the Poisson rain model of Section II-D, the interference process, denoted by $I_i(t)$, during the (unique) transmission of node X_i conforms to the above representation (3.2) with $\Phi^1(n)$ replaced by $\Psi^1(t) = \{X_j \in \Psi : e_j(t) = 1\}$, and $F_j^i(n)$ replaced by F_j^i .

Below, we propose two different ways of taking into account the variation of the interference during the packet reception.

- Consider the *maximal interference value* during the given transmission $I_i^{\max}(n) = \max_{t \in [T_i(n), T_i(n)+B]} I_i(n, t)$ or $I_i^{\max} = \max_{t \in [T_i, T_i+B]} I_i(t)$ for the Poisson-renewal or the Poisson rain model, respectively. This choice corresponds to the situation where bits of information sent within one given packet are not repeated/interleaved so that the interference needs to be controlled (e.g. through the SINR condition, see Section IV) at any time of the packet transmission (for all symbols) for the reception to be successful.
- Taking the *averaged interference value* over the whole packet duration $I_i^{mean}(n) = 1/B \int_{T_i(n)}^{T_i(n)+B} I_i(n, t) dt$ or $I_i^{mean} = \int_{T_i}^{T_i+B} I_i(t) dt$ for the Poisson-renewal or the rain model, respectively, corresponds to a situation where some coding with repetition and interleaving of bits on the whole packet duration is used.

In what follows we will be able to express, in closed form expressions, the Laplace transform of the averaged interference in our non-slotted models.

C. Laplace transform of the interference

In what follows we consider the interference experienced by an “extra” receiver added to the network (say at the origin) during the reception of a virtual packet which starts at time 0. In slotted Aloha, this will be just the interference I received at the origin during slot 0. For non-slotted Aloha, this will be the interference I^{mean} empirically averaged over the time interval $[0, B]$.

The general expression of the Laplace transform \mathcal{L}_I of I in the slotted Aloha scheme has already been studied. Here we recall the result assuming a general fading law, cf [4, 7, 9].

Proposition 3.1: *For the slotted Aloha model with path-loss function (3.1) and a general distribution of*

fading F with mean 1, we have

$$\mathcal{L}_I(\xi) = \exp\{-\lambda_p A^{-2} \xi^{2/\beta} \kappa_{\text{slotted}} \mathbf{E}[F^{\frac{2}{\beta}}]\}, \quad (3.3)$$

where $\kappa_{\text{slotted}} = \pi\Gamma(1 - 2/\beta)$ is called the spatial contention factor for slotted Aloha¹. In particular

- $\mathbf{E}[F^{\frac{2}{\beta}}] = 1$ in the no-fading scenario $F \equiv 1$,
- $\mathbf{E}[F^{\frac{2}{\beta}}] = 2\Gamma(2/\beta)/\beta$ with Rayleigh fading (F exponential) and $\mu = 1$.
- $\mathbf{E}[F^{\frac{2}{\beta}}] = \exp(\sigma^2(2 - \beta)/\beta^2)$ with F log-normal shadow-fading of mean 1².
- $\mathbf{E}[F^{\frac{2}{\beta}}] = \frac{\Gamma(k+2/\beta)}{\Gamma(k)2^{2/\beta}}$ with F a Nakagami distribution³.

Regarding the distribution of the averaged interference I^{mean} in non-slotted Aloha, we have the following new general result.

Proposition 3.2: *Let us consider the Poisson rain model of non-slotted Aloha with space-time intensity of packet transmissions $\lambda_s = \lambda\tau$ and the path-loss function (3.1). Let us assume a general distribution of fading F . Then the Laplace transform $\mathcal{L}_{I^{\text{mean}}}(\xi)$ of the averaged interference I^{mean} is given by (3.3) with the spatial contention factor $\kappa = \kappa_{\text{non-slotted}}$ equal to:*

$$\kappa_{\text{non-slotted}} = \frac{2\beta}{2 + \beta} \kappa_{\text{slotted}},$$

where κ_{slotted} is the spatial contention factor evaluated for slotted Aloha under the same channel assumptions.

Proof:

By (3.2) and by the definition of I^{mean} (regarding the interference experienced by an extra receiver added to the network at the origin during the reception of a virtual packet which starts at time 0), if we exchange the order of integration and summation we can express I^{mean} in the following form:

$$I^{\text{mean}} = \sum_{X_j \in \Phi} F_j^0 H_j / l(|X_j|),$$

where $H_j = \frac{1}{B} \int_0^B \mathbf{1}(X_j \text{ emits at time } t) dt$. In the Poisson rain model we have $\mathbf{1}(X_j \text{ emits at time } t) = \mathbf{1}(t - B \leq T_j \leq t)$, where T_j is the time at which X_j starts emitting. Integrating the previous function we obtain $H_j = h(T_j)$, where $h(s) = (B - |s|)^+/B$ and $t^+ = \max(0, t)$. Consequently, for the Poisson rain model represented by Poisson p.p. $\Psi = \{X_i, T_i\}$ (cf. Section II-D) the averaged interference at the typical transmission receiver is equal in distribution to:

$$I^{\text{mean}} \stackrel{\text{distr.}}{=} \sum_{X_j, T_j \in \Psi} F_j^0 h(T_j) / l(|X_j|),$$

¹The term spatial contention factor was introduced in [12].

² $F = \exp(-\sigma^2/2 + \sigma Z)$ with Z standard normal random variable.

³the density of F is $f(x, k) = \frac{k^k}{\Gamma(k)} x^{k-1} e^{-kx}$, note that this corresponds to Nakagami $(k, 1)$ fading.

where F_j^0 are i.i.d. copies of the fading. Using the general expression for the Laplace transform of the Poisson shot-noise (see e.g. [2, Prop. 2.2.4]), for the path-loss function (3.1) we obtain:

$$\mathcal{L}_{I^{\text{mean}}}(\xi) = \exp\left\{-2\pi\lambda_s \int_{-\infty}^{\infty} \int_0^{\infty} r \left(1 - \mathcal{L}_F(\xi h(t)(Ar)^{-\beta})\right) dr dt\right\},$$

where \mathcal{L}_F is the Laplace transform of F . Substituting $r := Ar(\xi h(t))^{-1/\beta}$ for a given fixed t in the inner integral we factorize the two integrals and obtain $\mathcal{L}_{I^{\text{mean}}}(\xi) = \exp\{\lambda_s A^{-2} \xi^{2/\beta} \zeta \eta\}$, where $\zeta = \int_{-\infty}^{\infty} (h(t))^{2/\beta} dt$ and $\eta = 2\pi \int_0^{\infty} r(1 - \mathcal{L}_F(r^{-\beta})) dr = \kappa_{\text{slotted}} \mathbf{E}[F^{\frac{2}{\beta}}]$. A direct calculation yields $\zeta = 2\beta/(2 + \beta)$. This completes the proof. ■

Remark 3.3: Recall that

$$\zeta = \zeta(\beta) = \frac{\kappa_{\text{non-slotted}}}{\kappa_{\text{slotted}}} = 2\beta/(2 + \beta)$$

is the ratio of the spatial contention parameters between non-slotted and slotted Aloha models. It can be seen as the *contention cost of non-synchronization in Aloha* (cf Remark 4.5 below). We plot its value as a function of β in Figure 1. Note that in the free-space propagation model (where $\beta = 2$) it is equal to 1 (which means that the interference distribution in slotted and non-slotted Aloha are the same). Moreover, $\zeta(\beta)$ increases with the path-loss exponent and asymptotically (for $\beta = \infty$) approaches the value 2 (as conjectured in [8]).

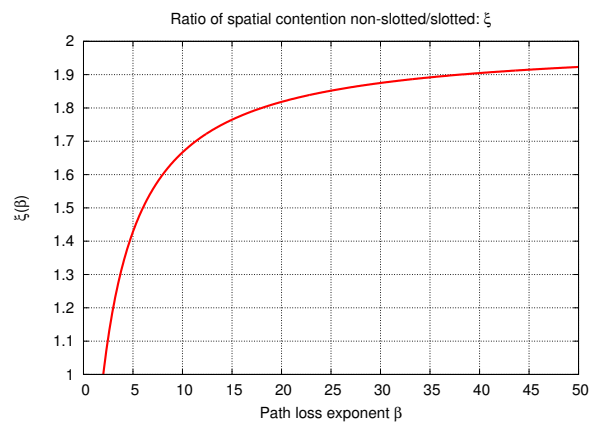


Fig. 1. Ratio of the spatial contention parameters between non-slotted and slotted Aloha models versus β .

D. Interference in the Poisson-Renewal Model

We now consider the mean interference $I^{\text{mean}} = I_0^{\text{mean}}(0)$ experienced by the receiver located at the origin 0, during the transmission of the packet, which starts at time $T_0 = 0$.

Proposition 3.4: *The Laplace transform of the interference I^{mean} in the Poisson-renewal model with arbi-*

rary distribution of fading F satisfying $\mathbf{E}[F^{2/\beta}] < \infty$ is given by the following expression:

$$\begin{aligned} \mathcal{L}_I^{mean}(\xi) = \exp \left[- \int_0^\infty \left(1 - \frac{\epsilon B(e^{-\xi/v} - e^{-B\epsilon})}{(1 + \epsilon B)(\epsilon B - \xi/v)} \right. \right. \\ \left. \left. - \frac{(\epsilon B)^2}{(1 + \epsilon B)(\xi/v - \epsilon B)} \int_0^1 e^{\epsilon B t} (1 - e^{(\xi/v - \epsilon B)(t-1)}) \tilde{\mathcal{L}}(\xi t/v) dt \right. \right. \\ \left. \left. - \frac{\epsilon B e^{-\epsilon B}}{(1 + \epsilon B)} \int_0^1 e^{\epsilon B t} \tilde{\mathcal{L}}(\xi t/v) dt - \frac{e^{-\epsilon B}}{(1 + \epsilon B)} \right) \Lambda(dv) \right], \end{aligned}$$

where

$$\begin{aligned} \Lambda(dv) &= \frac{2\lambda\pi\mathbf{E}[F^{2/\beta}]}{A^2\beta} v^{\beta/2-1} dv \\ \tilde{\mathcal{L}}(\eta) &= \frac{1}{\mathbf{E}[F^{2/\beta}]} \mathbf{E}[F'^{2/\beta} \mathcal{L}_F(\eta/F')] \end{aligned}$$

F and F' being independent with the law of the fading.

The proof of this proposition is given in the Appendix. The following two results consider two special cases: constant ($F \equiv 1$) and Rayleigh (F exponential) fading.

Proposition 3.5: Under the assumptions of Proposition 3.4, with $F \equiv 1$

$$\mathcal{L}_{I^{mean}}(\xi) = \exp \left\{ - \frac{2\pi\lambda}{A^2\beta} \int_0^\infty i(\xi/v) v^{2/\beta-1} dv \right\}$$

with

$$\begin{aligned} i(\xi/v) &= 1 - \frac{e^{-\epsilon B}(\epsilon B e^{\epsilon B - \xi/v} - \xi/v)}{(1 + \epsilon B)(\epsilon B - \xi/v)} \\ &- \frac{\epsilon B(\epsilon^2 B^2 e^{-\xi/v} - \epsilon B e^{-\xi/v} \xi/v - e^{-\xi/v} \xi/v + e^{-\epsilon B} \xi/v)}{(1 + \epsilon B)(\epsilon B - \xi/v)^2} \end{aligned}$$

Proof: When $F \equiv 1$ we have $\tilde{\mathcal{L}}(\eta) = e^{-\eta}$ and $\Lambda(dv) = \frac{2\lambda\pi}{A^2\beta} v^{\beta/2-1} dv$. Inserting the values of $\tilde{\mathcal{L}}(\eta)$ and $\Lambda(dv)$ in the expression given in Proposition 3.4 and after some algebra, one obtains the result. ■

Proposition 3.6: Under the assumptions of Proposition 3.4, with exponential fading F of mean 1 (which corresponds to Rayleigh fading) we have:

$$\begin{aligned} \mathcal{L}_{I^{mean}}(\xi) = \exp \left\{ -\lambda \int_{x \in \mathbb{R}^2} \left(1 - \frac{1}{1 + \epsilon B} \int_0^\infty \frac{\epsilon e^{-\epsilon s}}{1 + \frac{(B-s)+\xi}{Bl(|x|)}} ds \right. \right. \\ \left. \left. - \frac{\epsilon B}{1 + \epsilon B} \frac{1}{B} \int_0^B \frac{1}{1 + \frac{(B-t)\xi}{Bl(|x|)}} \int_0^\infty \frac{\epsilon e^{-\epsilon s}}{1 + \frac{(t-s)+\xi}{Bl(|x|)}} ds dt \right) dx \right\}. \end{aligned}$$

The proof of this formula can be found in [8].

IV. SINR COVERAGE ANALYSIS

In the slotted Aloha model it is natural to assume that transmitter X_i covers its receiver y_i in time slot n if

$$\text{SINR}_i(n) = \frac{F_i^i(n)/l(|X_i - y_i|)}{W + I_i(n)} \geq T, \quad (4.4)$$

where T is some SINR threshold. When condition (4.4) is satisfied we say that X_i can be successfully received by y_i or, equivalently, that y_i is not in outage with respect to X_i in time slot n . We will say that in non-slotted Aloha with maximal interference constraint, X_i can be successfully received by y_i (in time slot n in the case of the Poisson-renewal model), if condition (4.4) holds with $I_i(n)$ replaced by $I_i^{\max}(n)$ or I_i^{\max} in the Poisson-renewal or the Poisson rain models, respectively. Similarly, we will say that in non-slotted Aloha with average interference constraint, X_i can be successfully received by y_i (in time slot n in the case of the Poisson-renewal model), if condition (4.4) holds with $I_i(n)$ replaced by $I_i^{mean}(n)$ or I_i^{mean} in the Poisson-renewal or Poisson rain models, respectively.

We will see that the coverage probability with the average interference constraint (in both the Poisson-renewal and the Poisson rain model), can be easily derived from the Laplace transform of interference I^{mean} . We have not been able to derive closed formulas when the maximal interference constraint is used; this case is studied by simulations in Section V.

A. Coverage probability

Let us define the coverage probability p_c in the three models considered as the probability that the SINR value in the typical transmission exceeds the threshold T . More formally, we have

$$\begin{aligned} p_c &:= \mathbf{P}^{(0,0)} \{ \text{SINR}_0(0) \geq T \} \\ &= \mathbf{P}^{(0,0)} \{ F_0^0(0) \geq l(r)T(W + I_0(0)) \} \end{aligned}$$

where $\mathbf{P}^{(0,0)}$ denotes the Palm probability of Φ (given a node $X_0 = 0$ at the origin) and given that it starts its transmission at time 0 (indexed by $n = 0$), and where $I_0(0) = I_0^{mean}(0)$ for the non-slotted case.

Result 4.1: For the slotted and Poisson-rain non-slotted Aloha models with the path-loss function (3.1) and Rayleigh fading of mean $1/\mu = 1$, we have

$$p_c = \exp \left\{ -\lambda \tau r^2 T^{2/\beta} \kappa \right\}, \quad (4.5)$$

where

$$\begin{aligned} -\kappa &= \kappa_{\text{slotted}} \Gamma(2/\beta + 1) = \pi \Gamma(1 - 2/\beta) \Gamma(1 + 2/\beta) / \beta = \\ &= 2\pi \Gamma(2/\beta) \Gamma(1 - 2/\beta) / \beta \text{ and } \tau = p \text{ for slotted Aloha,} \\ -\kappa &= \kappa_{\text{non-slotted}} \Gamma(2/\beta + 1) = 4\pi \Gamma(2/\beta) \Gamma(1 - \\ &= 2/\beta) / (2 + \beta) \text{ for the non-slotted Poisson Aloha model.} \end{aligned}$$

Proof: The basic observation allowing explicit analysis of the coverage probability for all our Poisson models of Aloha is that the distribution of the interference $I_0(0)$ and $I_0^{mean}(0)$ and under $\mathbf{P}^{(0,0)}$ is independent of W and $F_0^0(0)$, and corresponds to the distribution of the interference “experienced” by an extra receiver in the respective model, studied in Section III. This is a consequence of Slivnyak’s theorem; cf. [2, Theorem 1.4.5]. Consequently, for all three (slotted, non-slotted rain or renewal) Aloha models, in the special case of Rayleigh fading we have $p_c = \mathcal{L}_W(Tl(r))\mathcal{L}_I(Tl(r))$, where I is the interference in the respective model ($I = I^{mean}$ for the non-slotted models). By Propositions 3.1 and 3.2 we have the above result. ■

For a general distribution of fading the evaluation of p_c from the Laplace transform \mathcal{L}_I (or $\mathcal{L}_{I^{mean}}$) is not so straightforward. Some integral formula, based on the Plancherel-Parseval theorem, was proposed in [5] when F has a square integrable density. This approach however does not apply to the no-fading case $F \equiv 1$. Here we suggest another, numerical approach, based on the Bromwich contour inversion integral and developed in [1], which is particularly efficient in this case.

Proposition 4.2: *For the (slotted, non-slotted rain and renewal) Aloha model with constant fading $F \equiv 1$ we have*

$$p_c = \frac{2 \exp\{\delta/(Tl(r))\}}{\pi} \int_0^\infty \mathcal{R}\left(\frac{1 - \mathcal{L}_I(\delta + iu)}{\delta + iu}\right) \cos(uT) du, \quad (4.6)$$

where $\delta > 0$ is an arbitrary constant and $\mathcal{R}(z)$ denotes the real part of the complex number z , with \mathcal{L}_I being the Laplace transform of the (mean) interference in the respective Aloha model.

As stated in [1], the integral in (4.6) can be numerically evaluated using the trapezoidal rule and the Euler summation rule can be used to truncate the infinite series; the authors also explain how to set $f\delta$ in order to control the approximation error.

B. Space-time efficiency

Spatial density of successful transmission is usually defined as the average number of successful transmissions per unit of time and space. This performance characteristic, introduced in [4] and widely accepted since then, can be considered as a measure of spatial throughput of the network. We will use this term in this paper. By the standard Campbell average formula, the spatial throughput is $d = \lambda\tau p_c$.

In what follows we optimize and compare this quantity for slotted and non-slotted Poisson-rain Aloha models assuming exponential Rayleigh fading.

The following result follows immediately from (4.1).

Proposition 4.3: *We assume that there is no noise $W = 0$, Rayleigh fading and path-loss (3.1). The maximum value of the spatial throughput is $d_{max} = 1/(er^2T^{2/\beta}\kappa)$ in slotted and non-slotted rain Aloha. This maximum is attained for the space-time density of channel access $\lambda\tau = 1/r^2T^{2/\beta}\kappa$. Moreover, given the spatial density of nodes λ the optimal mean channel-access-time-fraction τ per node τ_{max} for d_{suc} is equal to*

$$\tau_{max} = \frac{1}{\lambda r^2 T^{2/\beta} \kappa}.$$

if $\lambda > 1/r^2T^{2/\beta}\kappa$ and 1 (interpreted as no back-off; i.e., immediate retransmission) otherwise.

Remark 4.4: Since κ is larger for non-slotted Poisson rain Aloha than for slotted Aloha when we optimally tune the two protocols we have $\tau_{max}^{slotted} > \tau_{max}^{non-slotted}$. This means that optimally tuned non-slotted Aloha occupies less channel than optimally tuned slotted Aloha.

The following result compares the spatial throughput for slotted and non-slotted Aloha, when both are optimized

Proposition 4.5: *Under the assumptions of Result 4.3, the ratio of the spatial throughput for slotted and non-slotted Poisson rain Aloha is:*

$$\frac{d_{max}^{slotted}}{d_{max}^{non-slotted}} = \frac{\kappa_{non-slotted}}{\kappa_{slotted}} = \frac{1}{\zeta(\beta)} = \frac{2\beta}{\beta + 2}.$$

In Figure 4 we present this good-put ratio for the optimized systems as a function of β (note that it does not depend on other parameters such as λ, r, T). We observe that for small values of path-loss exponent β (close to 2) the performances of slotted and non-slotted Aloha are similar, but for large values of β non-slotted Aloha performs significantly worse than slotted Aloha. However even for $\beta = 6$ the ratio still remains significantly larger than 50% foreseen by the ‘well-known’ (simplified collision) model (See [6, Section 4.2]).

C. Energy efficiency

Note that both slotted Aloha and non-slotted Aloha (in the rain model), when optimally tuned for the spatial throughput $\tau = \tau_{max}$, have the same probability of successful transmission $p_c = 1/e$. This means that both schemes exhibit the same energy efficiency. If one assumes that each transmission requires one energy unit, the number of successful transmissions per unit of energy consumed is $p_c = 1/e$. Let us remark that this comparison does not take into account the energy used to maintain synchronization in the slotted scheme. Taking this fact into account we can say that non-slotted Aloha outperforms slotted Aloha in terms of energy efficiency.

V. NUMERICAL RESULTS

In this section we validate our models by comparing them with simulation results. The simulations are performed with random locations of the nodes drawn at the beginning of the simulation but not re-drawn at each transmission. Thus, in principle, the simulations are more aligned with the Poisson renewal model. We also compare the performance of slotted and non-slotted Aloha. If not otherwise defined we use the following numerical assumptions : $\lambda = 1$, $r = 1$, $T = 10$ and $\beta = 4$. The simulations are carried out in a square of $300 \text{ m} \times 300 \text{ m}$ with the same numerical assumptions. Let us recall that λ is the node density, $r = 1$ is the mean distance between the sender and receiver node, $T = 10$ is the capture threshold and $\beta = 4$ is the path-loss exponent. We use $r = 1$ which is, in this network, twice the mean distance from the current node to its closest neighbor, $T = 10$ is a default assumption when no coding (or other advanced technique) is used. The assumption $\beta = 4$ corresponds to the path-loss observed in dense urban scenarios.

A. Non-slotted Aloha, Renewal versus Rain model

In this section we validate our Poisson rain and renewal models by comparing the spatial throughput $\lambda\tau p_c$ obtained with these two models and with simulations. We adopt Rayleigh fading. For the rain model we have a closed formula but for the renewal model p_c is evaluated numerically using Proposition 4.2 and the Laplace transform derived from Proposition 3.4. We use the same numerical assumptions as previously: $\lambda = 1$, $r = 1$, $T = 10$ and $\beta = 4$. In Figure 2 we observe a very good matching of the two models with simulations. As already stated we are interested in scenarios with low mobility. Thus, in the simulations, the nodes' locations are not re-sampled at each transmission and the simulations are closer to the Poisson renewal model than to the Poisson rain model. Simulations with high mobility closer to the Poisson rain model are not presented in Figure 2) as they would have been aligned given with the Poisson Rain model.

We perform the same comparison between the two models and the simulations for $\beta = 5$ and $\beta = 3$. For $\beta = 5$ the matching of the two models and the simulation is perfect. For $\beta = 3$ the two models provide the same results whereas the simulations give a larger spatial of throughput. This can be explained by the fact that the simulation network is of finite length, and the border effects have a stronger impact for small values of β .

We then compare the Poisson rain and renewal models with no fading i.e. $F \equiv 1$. The result of this comparison is shown in Figure 3. We vary λ from 1 to 100 in the renewal model. We observe that the rain and the renewal

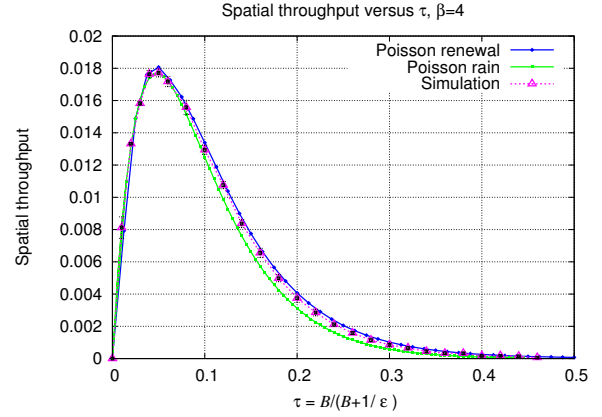


Fig. 2. Spatial throughput versus $\tau = \frac{B}{B+1/\epsilon}$. Comparison of the Poisson-renewal and the Poisson rain models with simulation results. Rayleigh fading.

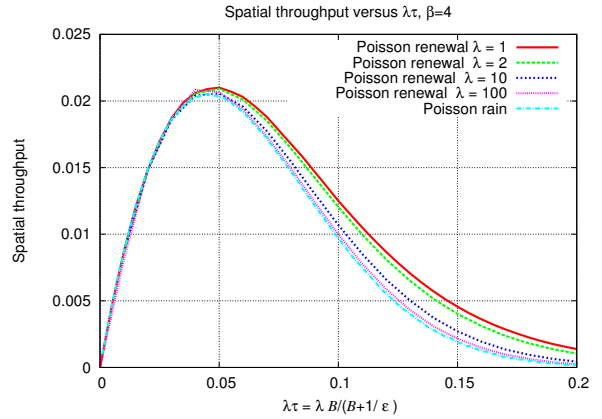


Fig. 3. Spatial throughput versus $\tau = \frac{B}{B+1/\epsilon}$. Convergence of the Poisson-renewal model towards the Poisson rain model.

models for $\lambda = 100$ show similar performances. This is because when λ is large, the transmitting node changes at every transmission, which is very close to the Poisson rain model. For small values of λ the two models show slightly different results.

B. Slotted versus non slotted Aloha

In Figure 4, we present the ratio of spatial throughput transmissions for non-slotted Aloha and slotted Aloha. We use the analytical model of slotted-Aloha and the Poisson rain model for non-slotted Aloha. We optimize non-slotted Aloha and slotted Aloha with respect to p and τ . We observe that for small values of the path loss exponent (close to 2) the performances of slotted and non-slotted Aloha are similar, but for large values of β slotted Aloha significantly outperforms non-slotted Aloha.

In Figure 5 we compare the spatial throughput for slotted Aloha and non-slotted Aloha when $\tau = p = \frac{\epsilon}{1+\epsilon} = 0.05$. We observe that for small values of the path loss exponent (close to 2) the performances of slotted

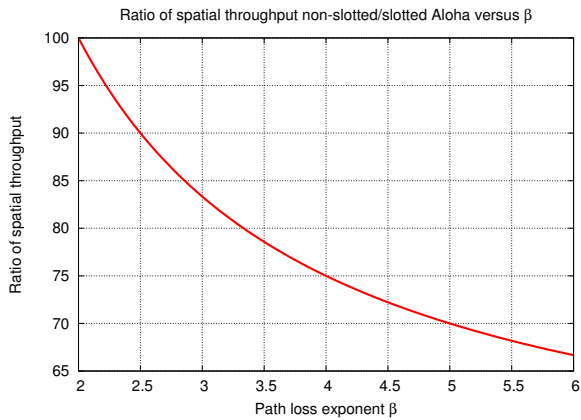


Fig. 4. The ratio (in %) of the good-put offered by non-slotted Aloha with respect to slotted Aloha, when both are optimized so as to maximize the spatial throughput as a function of the path loss exponent β . It is equal to the inverse of the contention cost $1/\zeta(\beta)$ and does not depend on any other parameter.

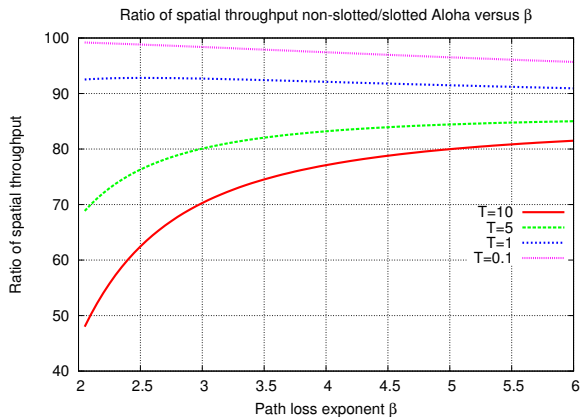


Fig. 5. The ratio (in %) of the good-put offered by non-slotted Aloha with respect to slotted Aloha, as a function of the path loss exponent β , for various choices of the SINR threshold T ; other parameters are $p = \frac{\epsilon}{1+\epsilon} = 0.05$, $\lambda = 1$, $r = 1$.

and non-slotted Aloha are similar when T is small but that slotted Aloha significantly outperforms non-slotted Aloha for medium to large values of T . For large values of T , slotted Aloha still outperforms non-slotted Aloha but the difference remains less than when T is small, non-slotted Aloha provides more than 80% of slotted Aloha throughput. We observe that in contrast to the case where the protocols are tuned to offer the maximum throughput, the ratio of throughput for non-slotted/slotted Aloha does depend on T (and of course on τ or p).

C. Mean Versus Maximum Interference Constraint in SINR

In this section, we show the impact of the assumption on the maximum interference constraint in the SINR on the probability of a successful transmission. In Figure 6, we compare the spatial throughput for non slotted Aloha,

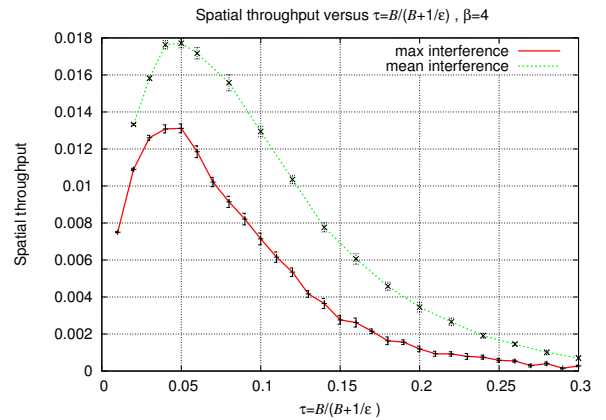


Fig. 6. Spatial throughput versus $\frac{B}{B+1/\epsilon}$ for mean and maximal interference constraint; simulation results.

we still have $\lambda = 1$, $r = 1$, $T = 10$ and $\beta = 4$. When the SINR is computed with the maximum interference instead of the mean interference the loss in performance is large and may be up to 45%. But if the throughput is optimized in ϵ , the loss in performance is only 26%. We observe that the throughput is optimized in both cases for the same value of $B\epsilon \simeq 0.045$, this value is also optimal for the Poisson rain model.

In Figure 7 we compare the spatial throughput for slotted Aloha and non-slotted Aloha when the maximum or average SINR is considered. For slotted Aloha, we use the analytical model and optimize spatial throughput in p . For non-slotted Aloha, we use simulation results and the Poisson rain model to optimize the schemes in $\frac{B}{B+1/\epsilon} = \tau$. We observe that for, $\beta \leq 4$ non-slotted Aloha with the averaged SINR provides 50% more throughput than with the maximum SINR. For $\beta \geq 5$, non-slotted Aloha with the averaged SINR provides only around 35% more throughput than with the maximum SINR. When we compare slotted Aloha with non-slotted Aloha with maximum SINR, we find that slotted Aloha offers 66% more throughput for $\beta = 3$ and 100% for $\beta = 6$.

VI. CONCLUSION

Following on from previous studies of slotted Aloha, we propose two models for pure Aloha: the Poisson rain and the Poisson renewal models. We provide simulation results to prove the validity of both models. We show that the Poisson renewal model converges towards the Poisson rain model when the density of nodes becomes large. As the main theoretical contribution we derive closed form expressions for the Laplace transform of the interference observed in both models with a general fading distribution. For the Poisson Rain model these expressions are very simple and particularly amenable to comparison with the previously well studied slotted Aloha model. Using this approach we express the gain in spatial

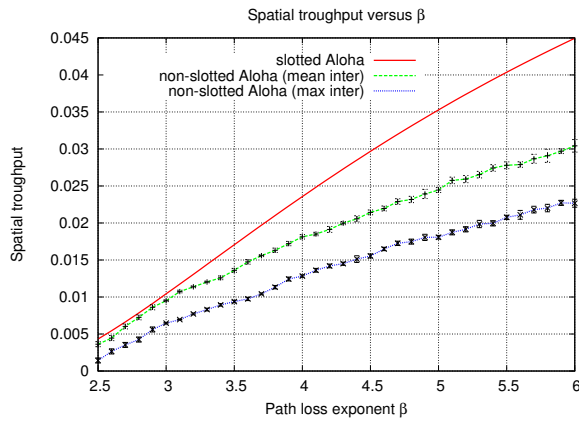


Fig. 7. Spatial throughput versus path loss exponent β . Slotted Aloha and non-slotted Aloha (mean and maximal interference constraint) are tuned to maximize the spatial throughput.

throughput for slotted Aloha (due to synchronisation) as a simple function of the path-loss exponent. It indicates that for small values of the path-loss exponent (close to 2) there is no gain from synchronisation, and that this gain very slowly increases with the increase in the path loss exponent (theoretically up to the factor of 2, when the path-loss exponent approaches infinity).

APPENDIX

A. Proof of Proposition 3.4

Each node X_j , $j \neq 0$, sends only two packets which can potentially interfere with the transmission of the packet of node $X_0 = 0$, which starts at time $T_0(0) = 0$. These are the last transmission (of X_j) which starts before time 0 (at time $T_j(0)$) and the first one which starts after time 0 (at time $T_j(1)$ with $T_j(0) \leq 0 < T_j(1)$). With this notation we have ⁴:

$$I^{mean} = \sum_{X_j \in \Phi} F_j^0(0)h(T_j(0))/l(|X_j|) + F_j^0(1)h(T_j(1))/l(|X_j|). \quad (1.7)$$

where $F_j^0(0)$ and $F_j^0(1)$ are the fading variables between station X_j and X_0 during the transmissions of the two potentially interfering packets described above. To simplify let us denote $F_j(0) = F_j^0(0)$, $F_j(1) = F_j^0(1)$, $H_j(0) = h(T_j(0))$, $H_j(1) = h(T_j(1))$. Let us consider the marked point process

$$\tilde{\Phi} = \{X_j, \left((F_j(0), F_j(1), H_j(0), H_j(1)) : j \neq 0 \right)\}.$$

It is an independently marked Poisson process with points $\{X_j : j \neq 0\}$, and marks $\{((F_j(0), F_j(1), H(0), H(1)))\}$ (independent across j , given points). Note that for given j , $F_j(0)$, $F_j(1)$ and the vector $(H_j(0), H_j(1))$ are mutually

independent, however, $H_j(0)$ and $H_j(1)$ are not independent from each other (we describe their joint distribution below). Let us consider the following mapping of $\tilde{\Phi}$

$$\tilde{\Psi} = \{(F_j(0)/l(X_j))^{-1}, \left((F_j(1)/l(X_j))^{-1}, H_j(0), H_j(1) \right)\}$$

considered again as a marked point process, with points $\{V_j := F_j(0)/l(X_j)\}^{-1}$ and marks $\left((F_j(1)/l(X_j))^{-1}, H_j(0), H_j(1) \right)$. By the displacement theorem it is again an independently marked Poisson point process, with intensity (of points) $\Lambda(0, s) = as^{2/\beta}$ where $a = \frac{\lambda\pi\mathbf{E}[F^{\frac{2}{\beta}}]}{A^2}$. Regarding its marks, $(H_j(0), H_j(1))$ are identically distributed vectors (as in $\tilde{\Phi}$). However, $(F_j(1)/l(X_j))^{-1}$, being independent of $(H_j(0), H_j(1))$, has a distribution which depends on the value of V_j . This distribution can be represented as follows: the law of $(F_j(1)/l(X_j))^{-1}$ given $V_j = v$ is equal to the law of $l(R_v)/F$ where

$$\mathbf{P}(R_v \leq r) = \frac{1}{\mathbf{E}[F^{\frac{2}{\beta}}]} \mathbf{E}[\mathbf{1}(F \leq \frac{l(r)}{v})F^{\frac{2}{\beta}}],$$

with F having the distribution of fading (hence the same as $F_j(0)$ and $F_j(1)$). Using these observations and the well known formula for the Laplace transform of the Poisson point process we obtain

$$\begin{aligned} \mathcal{L}_{I^{mean}}(\xi) &= \mathbf{E}[e^{-\xi I}] \\ &= \exp\left(-\int_0^\infty \left(1 - \mathbf{E}\left[\frac{H(0)}{v} + \frac{H(1)F}{l(R_v)}\right]\right)\Lambda(dv)\right). \end{aligned}$$

We focus now on the joint distribution of $(H(0), H(1))$ ⁵. Let $U[x, y]$ be the uniform law on $[x, y]$ and ϵ_0, ϵ_1 two independent exponential variables of rate ϵ . According to the renewal theory (see e.g. [3, eq. 1.4.3]), we have the following result. $T(0) = U[-B, 0]$ with probability $\frac{\epsilon B}{1+\epsilon B}$ and $T(0) = -(B + \epsilon_0)$ with probability $\frac{1}{1+\epsilon B}$. $T(1) = B + T(0) + \epsilon_1$ if $T(0) > -B$ and $T(1) = \epsilon_1$ otherwise. Thus we have $H(0) = h(-U)$ and $H(1) = h(-U + B + \epsilon_1)$ with probability $\frac{\epsilon B}{1+\epsilon B}$ and $H(0) = h(-U - \epsilon_0)$ and $H(1) = h(\epsilon_1)$ with probability $\frac{1}{1+\epsilon B}$, where U is $U[0, B]$. Consequently,

$$\begin{aligned} &\mathbf{E}\left[\mathbf{E}\left[e^{-\xi\left(\frac{H(0)}{v} + \frac{H(1)F}{l(R_v)}\right)} \mid H(0), H(1)\right]\right] \\ &= \mathbf{E}\left[e^{-\xi\frac{H(0)}{v}} \mathcal{L}_{F/lR_v}(\xi H(1))\right] \\ &= \frac{\epsilon B}{1 + \epsilon B} \mathbf{E}\left[e^{-\xi\frac{h(-U)}{v}} \mathcal{L}_{F/lR_v}(\xi h(-U + B + \epsilon_1))\right] \\ &\quad + \frac{1}{1 + \epsilon B} \mathbf{E}\left[e^{-\xi\frac{h(-B-\epsilon_0)}{v}} \mathcal{L}_{F/lR_v}(\xi h(\epsilon_1))\right] \end{aligned}$$

where

$$\mathcal{L}_{F/lR_v}(\xi) = \mathbf{E}\left[\mathbf{E}\left[e^{-\xi F/l(R_v)}\right]\right]$$

⁴We have: $h(s) = (B - |s|)^+/B$, see Proposition 3.2.

⁵we simplify the notation $H(0) = H_j(0)$, $H(1) = H_j(1)$

$$= \mathbf{E}[F'^{2/\beta} e^{-\xi F'/l(vF')^{1/\beta}}].$$

with F' being independent of F with the same distribution. Note that $\mathcal{L}_{F'/lR_v}(\xi) = \tilde{\mathcal{L}}(\xi/v)$, where $\tilde{\mathcal{L}}(\xi) = \mathbf{E}[F'^{2/\beta} \mathcal{L}_F(\xi/F')]$. Thus, we have:

$$\begin{aligned} & \mathbf{E}[\mathbf{E}[e^{-\xi(\frac{H(0)}{v} + \frac{H(1)F}{l(Rv)})} | H(0), H(1)]]] \\ &= \frac{\epsilon B}{(1 + \epsilon B)B} \int_0^B e^{-\xi h(-u)/v} \mathbf{E}[\tilde{\mathcal{L}}(\xi h(-u + B + \epsilon_1)/v)] du \\ & \quad + \frac{1}{1 + \epsilon B} \mathbf{E}[e^{-\xi h((-B - \epsilon_0)/v)}] \mathbf{E}[\tilde{\mathcal{L}}(\xi h(\epsilon_1)/v)] \\ &= \frac{\epsilon B}{(1 + \epsilon B)B} \int_0^B e^{-\xi h(-u)/v} \mathbf{E}[\tilde{\mathcal{L}}(\xi h(-u + B + \epsilon_1)/v)] du \\ & \quad + \frac{1}{1 + \epsilon B} \mathbf{E}[\tilde{\mathcal{L}}(\xi h(\epsilon_1)/v)]. \end{aligned}$$

We set :

$$\begin{aligned} E_1 &= \mathbf{E}[\tilde{\mathcal{L}}(\xi h(-u + B + \epsilon_1)/v)] \\ E_2 &= \mathbf{E}[\tilde{\mathcal{L}}(\xi h(\epsilon_1)/v)] \\ F_1 &= \frac{1}{B} \int_0^B e^{-\xi h(-u)/v} E_1 du. \end{aligned}$$

Let us denote $\eta = \xi/v$ and calculate:

$$\begin{aligned} E_1 &= \epsilon \int_0^u e^{-\epsilon s} \tilde{\mathcal{L}}\left(\frac{\eta(u-s)}{B}\right) ds + e^{-\epsilon u} \\ E_2 &= \epsilon \int_0^B e^{-\epsilon s} \tilde{\mathcal{L}}\left(\frac{\eta(B-s)}{B}\right) ds + e^{-\epsilon B} \end{aligned}$$

and

$$\begin{aligned} F_1 &= \frac{\epsilon}{B} \int_0^B e^{-\eta(1-u/B)} \int_0^u e^{-\epsilon s} \tilde{\mathcal{L}}\left(\frac{\eta(u-s)}{B}\right) ds du \\ & \quad + \frac{1}{B} \int_0^B e^{-\eta(1-u/B)} e^{-\epsilon u} du. \end{aligned}$$

Using the change of variable $\frac{u-s}{B} = t$ we obtain:

$$\begin{aligned} F_1 &= \int_0^1 \frac{\epsilon B}{\eta - \epsilon B} (e^{\eta - \epsilon B} - e^{t\eta - t\epsilon B}) \mathcal{L}(\eta t) dt \\ & \quad + \frac{e^{-\eta}}{\epsilon B - \eta} (1 - e^{\eta - \epsilon B}) \\ &= \frac{\epsilon B e^{\eta - \epsilon B}}{\eta - \epsilon B} \int_0^1 e^{-\epsilon B t} (1 - e^{(\eta - \epsilon B)(t-1)}) \mathcal{L}(\eta t) dt \\ & \quad + \frac{e^{-\eta}}{\epsilon B - \eta} (1 - e^{\eta - \epsilon B}). \end{aligned}$$

Denoting

$$F_2 = E_2 = \epsilon B e^{-\epsilon B} \int_0^1 e^{t\epsilon B} \mathcal{L}(\eta t) dt + e^{-\epsilon B}$$

we have:

$$\begin{aligned} & \mathcal{L}_{I_{mean}}(\xi) \\ &= \exp\left[-\int_0^\infty \left(1 - \frac{\epsilon B}{(1 + \epsilon B)} F_1 - \frac{1}{(1 + \epsilon B)} F_2\right) \Lambda(dv)\right] \end{aligned}$$

which gives the result presented.

REFERENCES

- [1] J. Abate and W. Whitt. Numerical inversion of laplace transforms of probability distributions. *ORSA Journal on Computing*, 7(1):38–43, 1995.
- [2] F. Baccelli and B. Błaszczyszyn. *Stochastic Geometry and Wireless Networks, Volume I — Theory*, volume 3, No 3–4 of *Foundations and Trends in Networking*. NoW Publishers, 2009.
- [3] F. Baccelli and P. Bremaud. *Elements of Queueing Theory. Palm Martingale Calculus and Stochastic Recurrences*. Springer, 2003.
- [4] F. Baccelli, B. Błaszczyszyn, and P. Mühlethaler. An Aloha protocol for multihop mobile wireless networks. *IEEE Trans. Inf. Theory*, 52:421–436, 2006.
- [5] F. Baccelli, B. Błaszczyszyn, and P. Mühlethaler. Stochastic analysis of spatial and opportunistic Aloha. *IEEE JSAC, special issue on Stochastic Geometry and Random Graphs for Wireless Networks*, 2009.
- [6] D. Bertsekas and R. Gallager. *Data Networks*. Prentice-Hall, Englewood Cliffs, 2001.
- [7] B. Błaszczyszyn and Holger Paul Keeler. Equivalence and comparison of heterogeneous cellular networks. In *Proc. of PIMRC – WDN-CN*, 2013.
- [8] B. Błaszczyszyn and P. Mühlethaler. Stochastic analysis of non-slotted Aloha in wireless ad-hoc networks. In *Proc. of IEEE INFOCOM*, San Diego, CA, 2010.
- [9] B. Błaszczyszyn, M. Karray, and F. Klepper. Impact of the geometry, path-loss exponent and random shadowing on the mean interference factor in wireless cellular networks. In *Third Joint IFIP Wireless and Mobile Networking Conference (WMNC)*, 2010.
- [10] S. Ghez, S. Verdu, and S. Schartz. Stability properties of slotted Aloha with multipacket reception capability. *IEEE Trans. Automat. Contr.*, vol 7, pages 640–648, 1988.
- [11] EN Gilbert and HO Pollak. Amplitude distribution of shot noise. *Bell Syst. Tech. J.*, 39(2):333–350, 1960.
- [12] M. Haenggi. Outage, local throughput, and capacity of random wireless networks. *IEEE Trans. Wireless Comm.*, 8:4350–4359, 2009.

- [13] Steven B Lowen and Malvin Carl Teich. Power-law shot noise. *Information Theory, IEEE Transactions on*, 36(6):1302–1318, 1990.
- [14] Roberts and G. Lawrence. Outage probability in multiple access packet radio networks in the presence of fading. *Computer Communications Review*, 5(2):28–42, 1975. doi: 10.1145/1024916.1024920.
- [15] Elvino S. Sousa and John A. Silvester. Optimum transmission ranges in a direct-sequence spread-spectrum multihop packet radio network. *Selected Areas in Communications, IEEE Journal on*, 8(5): 762–771, 1990.
- [16] D. Tse and P. Viswanath. *Foundamentals of Wireless Communication*. Cambridge University Press, 2005.
- [17] Michele Zorzi and Silvano Pupolin. Outage probability in multiple access packet radio networks in the presence of fading. *Vehicular Technology, IEEE Transactions on*, 43(3):604–610, 1994.